An aptamer-functionalized chemomechanically modulated biomolecule catch-and-release system

Chemo-mechanically Modulated Biomolecule "Catch and Release" with Aptamer-functionalized Reconfigurable Systems

Ankita Shastri[1], Lynn McGregor[1], Ya Liu[2], Valerie Harris[3], Hanqing Nan[3], Maritza Mujica[3], Yolanda Vasquez[4], Amitabh Bhattacharya[2], Yongting Ma[2], Michael Aizenberg[5], Olga Kuksenok[2], Anna Balazs[2], Joanna Aizenberg[1,4,5]*, Ximin He[3,4]*

Affiliations

1. Department of Chemistry and Chemical Biology, Harvard University, Cambridge, MA, United States.
2. Department of Chemical and Petroleum Engineering, University of Pittsburgh, Pittsburgh, PA, United States.
3. Materials Science and Engineering, Biodesign Institute, School for Engineering of Matter, Transport and Energy, Arizona State University, Tempe, AZ, United States.
4. School of Engineering and Applied Science, Harvard University, Cambridge, MA, United States.
5. Wyss Institute for Biologically Inspired Engineering, Harvard University, Cambridge, MA, United States.

The efficient extraction of (bio)molecules from fluid mixtures is vital for applications ranging from target characterization in (bio)chemistry to environmental analysis and biomedical diagnostics. Inspired by biological processes that seamlessly synchronize the capture, transport and release of biomolecules, we designed a robust chemo-mechanical sorting system capable of the concerted "catch and release" of target biomolecules from a solution mixture. The hybrid system is composed of target-specific, reversible binding sites attached to microscopic fins embedded in a responsive hydrogel that moves the cargo between two chemically-distinct environments. To demonstrate the utility of the system, we focus on the effective separation of thrombin by synchronizing the pH-dependent binding strength of a thrombin-specific aptamer with volume changes of the pH-responsive hydrogel in a biphasic microfluidic regime, and show the non-destructive separation with quantitative sorting efficiency, system's stability and amenability to multiple solution recycling.

Numerous biological processes involve the synchronized trapping, transporting, and sorting of specific biomolecules within complex fluids.[1] These processes arise from a chemo-mechanically modulated inherent integration of molecular recognition, reconfiguration and micromechanical motion of components in response to various internal signals.[1, 2] In contrast, current techniques for biomolecule sorting often require significant, even destructive, biomolecule modification, many sequential steps, and high energy input from lasers, sources of electrical, IR, or magnetic fields.[3-8] Considerable effort has recently been devoted to developing dynamic micro- and nano-scale hybrid systems that exploit the precise geometry of their components, combine chemical and mechanical action, act in a multimodal fashion, and even generate autonomous movement or

autoregulation.[9-19] Such dynamic chemo-mechanical approaches, if applied to biomolecule detection and separation, could advance chemical and clinical technologies that focus on diagnostics and purification.

Here, we draw inspiration from the ability of vesicle-carrying kinesins and dyneins to shuttle different biomolecule cargoes along the microtubule network[20] to develop a conceptually new chemo-mechano-biochemically modulated system that performs sequential, self-regulated "catch-transport-release" of target biomolecules from one fluid flow to another. Critical components for our cooperative, hierarchical system include: (i) compartments that provide two chemically distinct environments; (ii) a stimuli-responsive affinity handle for the biomolecules that can bind the target in one environment and release it in another; (iii) a dynamic "arm" that moves the cargo between the two compartments; (iv) an "artificial muscle" that actuates the arm's motion.

In our system, the chemically distinct environments are produced *via* a microfluidic system that yields two parallel fluid streams undergoing laminar flow. Aptamers (short DNA, RNA or peptide molecules that recognize specific chemical targets) serve as the stimuli-responsive affinity handles due to their ability to reversibly bind target molecules in different environments.[21, 22] (For example, DNA aptamers can denature and refold to capture and release their targets in response to temperature or pH changes.) The dynamic arms are supplied by aptamer-decorated, polymeric microscopic fins that are embedded in a stimuli-responsive hydrogel, which undergoes significant volumetric changes in response to environmental cues and, thus, functions as the actuating "muscle" that drives the reversible bending of microstructures.[23-25] Importantly, the reversible aptamer folding and biomolecule binding are synchronized with the reversible volume changes of the hydrogels such that the polymeric microfins provide the coordinated transportation of cargo between the compartments in the microfluidic system and result in the efficient capture and separation of biomolecules. This design is distinct from conventional biomolecule sorting systems by its reliance on a concerted cascade of chemo-mechano-biochemical energy transduction, as opposed to isolated energy inputs in the form of laser, electrical, or magnetic fields.

An especially useful feature of this system is that the hydrogel and aptamer binding can be chosen to respond to the same stimulus, such as for example, pH changes. Aided by computational modeling, we assembled such a system and illustrated its ability to separate an exemplary biomolecule, thrombin, by coordinating the pH-sensitive affinity of the thrombin protein to its aptamer (5'-GGTTGGTGTGGTTGG-3')[26, 27] with the pH-sensitive contraction and expansion of the poly(acrylamide-*co*-acrylic acid) hydrogel (PAAc-*co*-PAAm). By immersing this hybrid assembly in a microfluidic system, under bilayer fluid flow, we achieved the efficient catch of thrombin from the ingoing mixture in the top layer and its subsequent release in the separate flow in the bottom layer. In this way, we exploited the pH-responsive chemo-mechano-biochemical modulations of the system to separate and collect thrombin from a mixture without the use of expensive and complex tools, suggesting great promise for point-of-care diagnosis, monitoring, drug testing, and sorting for cell-based therapeutics.[28-31]

Results and Discussion

To enable synchronized hydrogel actuation and target molecule catch and release in response to a single stimulus, we selected a hydrogel and an aptamer that both respond to changes in pH. We chose a well-characterized aptamer that specifically binds human α-thrombin, 5'-GGTTGGTGTGGTTGG-3', a serine protease that plays a key role in the blood-clotting cascade, at appropriate pH in the range of 6-7 (Fig.1a).[26, 27] Importantly, this aptamer is known to reversibly denature and lose affinity for thrombin at low pH (Fig.S1).[32] Similarly, PAAc-*co*-PAAm is a well-studied, biocompatible hydrogel that contracts at pH < pK_a=4.25 and swells at pH > pK_a (Fig.1b).[17] We anticipated that linking these two pH-responsive components with flexible epoxy microstructures (10μm width, 2μm length, 18μm height, 5μm spacing) in a microfluidic system (see SI Fig. S2.1 for more details) would enable selective and repetitive capture of active thrombin from a cocktail of molecules flowed in the top layer kept at constant pH, which corresponds to the highest binding efficiency of the aptamer. The target is released and collected in the bottom layer, facilitated by hydrogel volume change-induced microstructure bending, where the pH is alternated between basic and acidic conditions, as schematically presented in Fig.1c.

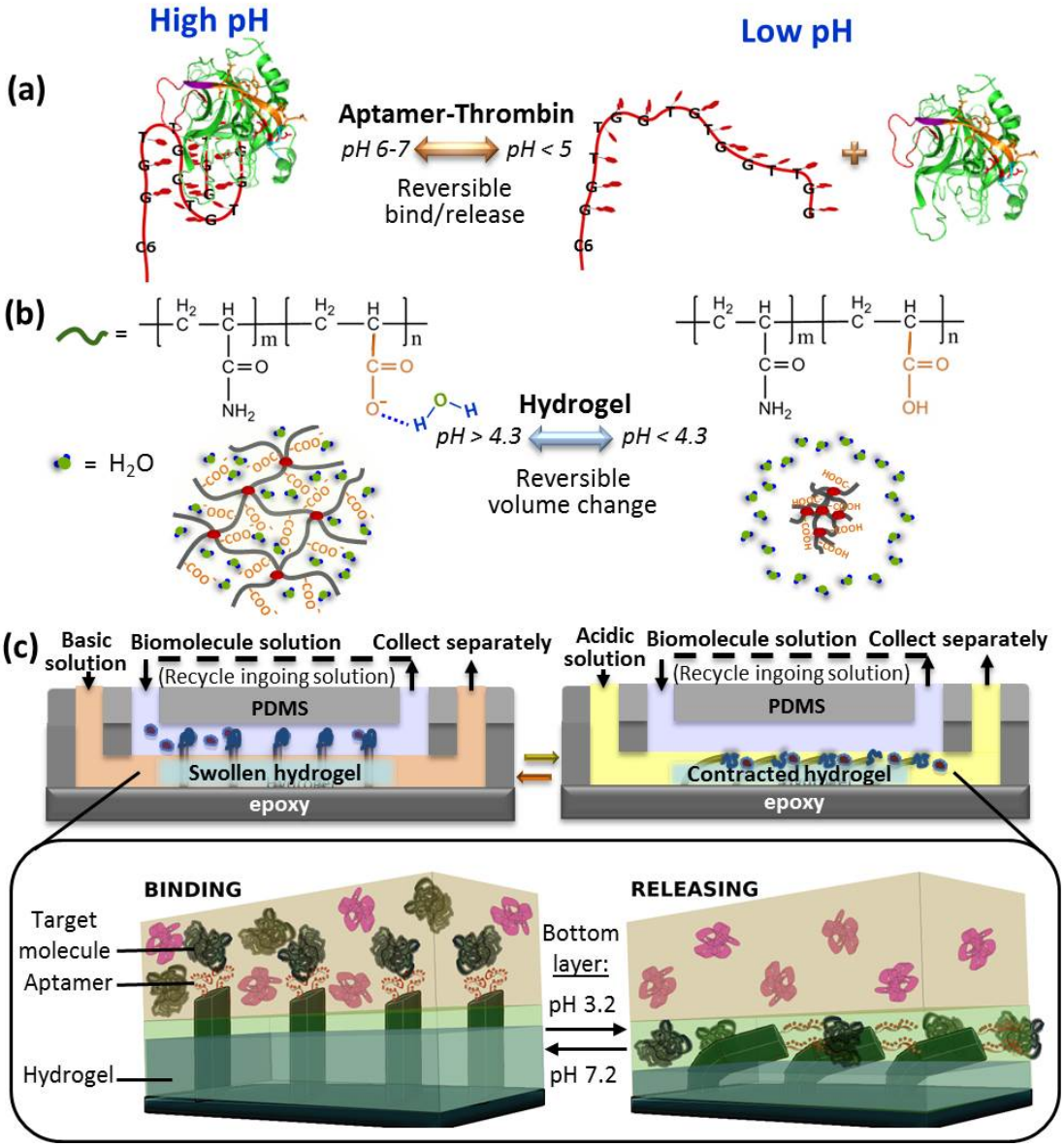

Figure 1. Design of the chemo-mechanically modulated biomolecule catch and release system by integrating the pH-responsiveness of the aptamer binding strength and the volume change of hydrogel into a pH-controlled reconfigurable microfluidic system. *(**a**) pH-dependent reversible binding and releasing of thrombin by DNA aptamer at pH=6-7 and pH<5 respectively due to the configuration change of the aptamer DNA strand. (**b**) pH-dependent reversible volume change of hydrogel (PAAc-co-PAAm), which swells at pH>pK_a=4.3, when the carboxylic groups are deprotonated leading to the absorbing of water into gel matrix, and expels water and contracts at pH<pK_a=4.3. (**c**) Scheme depicting a cross-sectional view of a biphasic microfluidic chamber under constant laminar flow with aptamer-decorated microstructures. The top fluid layer is used to introduce mixtures of biomolecules and is kept at constant physiological pH. In the presence of a solution of pH 7.2, the hydrogel in the bottom layer is swollen, and the aptamer-decorated microfins protrude into the top*

solution, exposing aptamers to the biomolecule mixture and binding the target biomolecule thrombin in the buffer of pH 6.3. In the presence of an acidic solution of pH 3.2, the hydrogel contracts, bending the aptamer-decorated microstructures into the bottom layer, which results in denaturation of the aptamer and release of captured thrombin molecules into the bottom layer. The bottom solution containing released target molecules can be collected separately from the top layer, enabling separation of target biomolecules from mixtures.

To gain insight into factors affecting the performance of this hybrid system, we first conducted computer simulations of the interactions among oscillating fins, target proteins, which are modeled as "adhesive nanoparticles", and non-target proteins, which are simulated as "nonadhesive particles" (see Supporting Information), to identify conditions when selective capture of the target adhesive nanoparticles from the upper mixed fluid stream is followed by their release into the lower stream, which is initially free of particles. To model the actuation, we impose a periodic motion on the fins, so that the angle θ between a fin and the lower wall varies sinusoidally with time between the values $\theta = \pi/2$ and $\theta = \theta_{low}$ with an angular frequency ω. We focus primarily on the first half of the oscillation cycle, corresponding to the contraction of the underlying gel. We apply a pressure gradient, ∇P, that drives the fluid from the left to the right along the microchannel and past the oscillating fins, as marked by the arrow in Fig.2a. We keep the fins stationary after they have reached θ_{low}, but continue to apply the pressure gradient. We assume that the interface between the two fluids remains at a constant position, h_{int}, as is consistent with previous experimental observations.[17, 33] When the fins are tilted at θ_{low}, their tips are below the interface h_{int} (Fig.2b). Importantly, only the fin sites that are located in the upper phase (above h_{int}) are assumed to be adhesive and able to form strong bonds with the adhesive nanoparticles. The binding between a fin site and nanoparticle is modeled through a Morse-potential, where the binding depends on the particle-fin separation.[34] These bonds are broken and the respective fins sites become nonadhesive to both types of nanoparticles if they are surrounded by the lower stream.

The simulations show (Fig.2c) that approximately 70% of the adhesive particles are captured from the upper stream and then released into the lower stream in a given simulation run, while less than 10% of the non-adhesive particles are drawn into the lower stream. This is evident from the respective time evolution curves $C(t)$ (blue and magenta

lines in Fig. 2c), which give the ratio between the numbers of nanoparticles of a given type in the lower phase to the total number of particles of the same type. This selective catch and release process can be understood from the evolution of the number of the bonds formed between the adhesive particles and adhesive fin sites (black line in Fig.2c). The number of bonds formed saturates even when the fins are in the upper fluid, due primarily to the number of *available* adhesive sites in the system. The number of adhesive sites effectively limits the maximum number of nanoparticles that can potentially be collected in one actuation cycle since each site on a fin can form only a single bond with the adhesive nanoparticle. The simulations clearly demonstrate the feasibility of the proposed synchronized capture and release and selective sorting of the biomolecules.

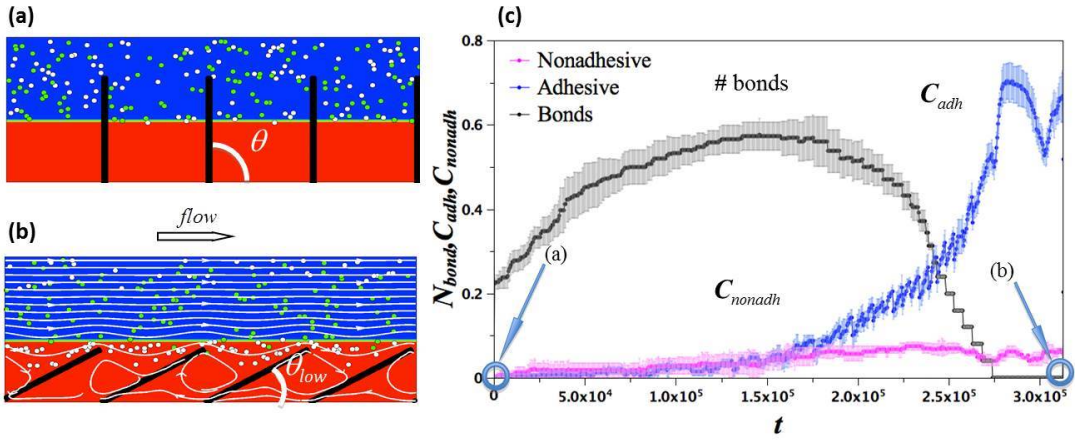

Figure 2. Computer simulations of the selective binding and release. *(a-b) Snapshots of the system at the onset of simulations at t=0 in (a) and at late times when the tilt angle between the fins and the bottom substrate is* $\theta_{low} = \pi/6$ *in (b). The fins are anchored to the floor of a two-dimensional microchannel and assumed to be actuated by an underlying chemo-responsive gel. After the fins reach the angle* θ_{low}*, we turn off the fins' motion, but continue to apply the pressure gradient. Adhesive particles are shown in white and non-adhesive particles are shown in green; the total number of particles is N=200 (100 of each type). The fluid streamlines are shown in white. (c) Evolution of the fraction of particles in the lower stream C(t) for adhesive particles (in blue) and non-adhesive particles (in magenta) and evolution of the number of bonds between the fins and the adhesive particles normalized by 100 (in black). The points marked (a) and (b) on the x-axis in (c) correspond to the respective snapshots (a) and (b). For simulation parameters and the relationship between the simulation and experimental values see Section 5.1 of SI.*

To experimentally realize this system, the microfluidic channel requires distinct inlets and outlets for the top and bottom layer to maintain independent control of the pH in each layer and to separate the target molecule from a complex ingoing mixture. The two fluid

layers are under constant laminar flow and effectively do not mix within the microfluidic channel or cause microstructure bending by itself (Fig.S2.1). The use of two separate inlets allows for control of the pH in each layer to create the chemically distinct environment for the concerted reconfigurations; the use of two separate outlets provides efficient sorting, without the need of washing steps to remove non-target proteins or separate elution steps to release the captured thrombin. Importantly, the dynamic chemo-mechanical response of the hydrogel to different pH in the bottom layer ensures the synchronized removal of the aptamer-bound thrombin from the top layer into the bottom layer with synchronized chemo-mechanical reconfiguration in a single step. Moreover, the ability to continuously separate the target molecule from the top layer allows for the recycling of the ingoing solution for multiple rounds, enabling separation of nearly all of the target molecules for high-efficiency biomolecule detection, isolation and purification.

To enable pH-regulated capture and release, we tested the pH dependence of thrombin-aptamer binding.[35, 36] Using an enzyme-linked oligonucleotide immunoassay (ELONA), we observed the highest thrombin-aptamer affinity at pH 6.3 (disassociation constant $K_{d,apparent} \cong 14.8$ nM), and thus, a buffer with pH 6.3 was used in the top layer where the aptamer-thrombin binding occurs (Fig.S1). A buffer with pH 7.2 was used in the bottom layer to swell the hydrogel and straighten the microstructures so that the aptamer-bearing tips would protrude into the top fluid for binding. Once thrombin is captured by the aptamer in the top layer, the release of the target into the bottom layer will occur at a pH that permits both fast and sufficient hydrogel contraction and aptamer reconfiguration to decrease binding to thrombin. An ELONA showed substantial reduction in the aptamer-thrombin affinity in decreasing pH from pH 6.3 to pH 5.0 ($K_{d,apparent}$=35nM) (Fig.S1). Since the onset of hydrogel contraction is at pH 4.3, we chose a buffer with pH 3.2 for the use in the bottom layer to ensure both the sufficient bending of the microstructures and dissociation of the bound thrombin, as depicted in Fig.1c.

Decoration of epoxy microfin tips with a DNA aptamer was verified by XPS (Fig. S2.2b) confocal microscopy, which detected fluorescence corresponding to a modified DNA strand complementary to the aptamer on the tips of functionalized microfins, but not on control microfins (Fig.S2.2). Fluorescently labeled thrombin was then flowed through the

microfluidic channel and subjected to one cycle of capture (bottom layer pH=7.2), transport, and release (bottom layer pH=3.2). Confocal microscopy demonstrated that thrombin was bound to the tips of the microfins when the bottom layer solution had pH 7.2, and was absent after the bottom layer was replaced with a solution of pH 3.2 (Fig.3a). In a control experiment, the fluorescence of the thrombin label remained unaffected by switching the pH from 6.3 to 3.2 (Fig.S3.1), thus validating the successful release of thrombin at pH 3.2. Importantly, released thrombin retained antibody binding activity comparable to untreated thrombin (Fig.S3.2). Computational simulation also shows the fluid continues to flow along the channel above the bent fins for smooth protein release and movement to the collection outlet (see SI Fig. S8). These results demonstrate that the microsystem enables concerted, non-destructive catch-transport-release of a target biomolecule, with the collected biomolecules remaining active and suitable for further use and analysis.

In order to systematically study and quantify the total binding capacity of the biomolecule sorting, as well as its effectiveness in capturing the target molecule, we injected into the device the same volume of solutions having increasing concentrations of thrombin (translating into 0.5, 1.0, 2.0, 4.0 and 8.0 picomoles total of thrombin), then proceeded through the release step, and collected and analyzed the bottom layer of outgoing solutions. The collected amount of thrombin increased with the increase in the injected amount and eventually leveled off, forming a plateau at ~0.7 picomole for 4.0 and 8.0 picomoles of ingoing thrombin (Fig.3b). This value represents the *maximum binding capacity* of the microfluidic sorting system with the given flow characteristics, dimensions of the channel, specific microfin area (0.5x8mm) available for aptamer functionalization and exposed to the top layer. Although there is a clear plateau, error in these measurements represents experiments conducted with 4 different microdevices with the same dimensions and volume, where differences could come from aptamer functionalization and measurement of thrombin with ELISA. This finite capacity correlates well with the simulations shown in Fig. 2 that suggest that no additional capture occurs when all adhesive sites are saturated. The sorting efficiency of the system can therefore be defined as the amount of target molecule captured, transported, and released in one

actuation cycle relative to the dimension- and flow-determined maximum binding capacity of the system (0.7 picomole in the current set-up) for various ingoing biomolecule concentrations (see Materials and Methods for details). Importantly, the same set of experiments utilizing either no aptamer on the fins or a mismatched sequence in place of the aptamer did not produce detectable levels of thrombin in the bottom effluent layer (Fig.3b). Taken together, these results proved the ability of our system to capture and release the target biomolecule from ingoing solutions having a broad range of concentrations. Furthermore, they demonstrated the robustness of the integrated chemistries of binding and release and their compatibility with the hydrodynamic/diffusion characteristics of the microfluidic sorting system.

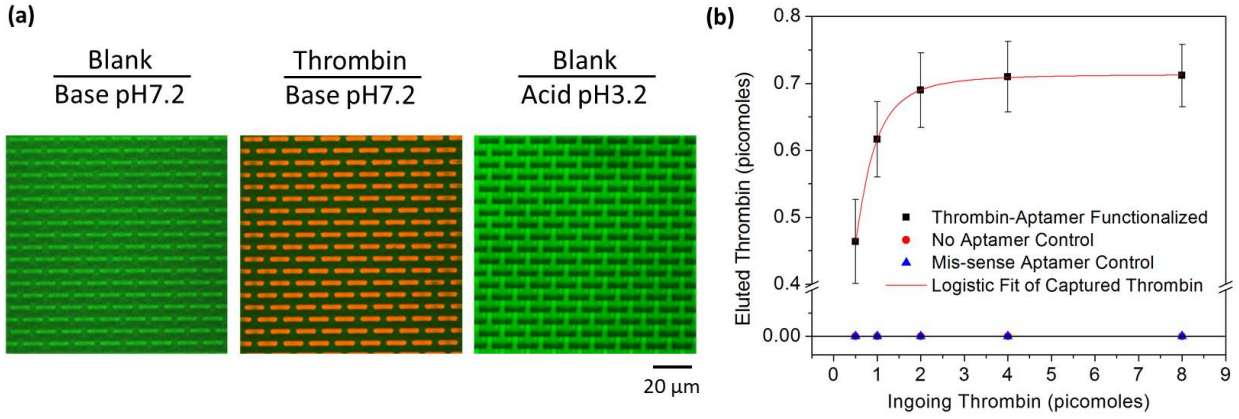

Figure 3. Capability of chemo-mechanically modulated sequential catch and release of thrombin in microfluidic system. *(a) Thrombin capture and release with microfins visualized by confocal microscope. Top view images of aptamer-decorated microstructure tips in biphasic microfluidic system. All images focus on the microstructure tips and are a composite of two wavelengths, 488 nm, used to visualize auto-fluorescence of the epoxy microstructures, and 543 nm, used to visualize Dylight dye-labeled thrombin. Left image: microstructures stand upright when basic buffer (pH 7.2) solution flows through the bottom layer. When a blank solution containing no thrombin is flowed in the top layer, only epoxy auto-fluorescence is detected. Middle image: Dylight dye-labeled thrombin is flowed through the top layer and is captured by the aptamer on the tips of the microstructures standing upright, while the fluid at bottom remains the basic buffer (pH 7.2) solution. Right image: introducing acidic buffer (pH 3.2) into the bottom layer bends the microstructures into bottom layer and releases Dylight dye-labeled thrombin from the aptamer-decorated microstructure tips, while the blank solution flows in the top layer. (b) Sorting Capacity of the Microfluidic System. Increasing quantities of thrombin were pumped into the top layer of the microfluidic channel with dimensions of 0.5mm x 8mm x 0.06mm. After microstructure bending, the bottom layer solution was collected and the eluted thrombin was quantified by ELISA. The amount of captured thrombin saturates at 0.71 picomoles, defining the sorting capacity. Error bar = standard deviation, n = 4.*

Most analytical applications require high levels of analyte separation and the ability to reuse the device multiple times. We anticipated that recycling the ingoing solution in our system would allow for recovery of the thrombin that was not captured in the previous cycles. Indeed, when a solution initially containing 2 picomoles of thrombin was introduced and recycled eight times through the microfluidic channel, the amount of recovered thrombin grew from ~0.7 after the first cycle to ~1.9 picomoles, thus reaching nearly 95.5% of the total ingoing thrombin (Fig.4a). This clearly demonstrates the system's robustness and efficacy in repeated catch-transport-release cycles.

Multiple actuation cycles were also examined in the computer simulations to probe the "capture-transport-release" dynamics associated with the repeated oscillations of the fins. Here, the peak values correspond to the microstructures bent into the lower phase when the fraction of adhesive particles in the lower phase is maximized. Qualitatively similar to experiments, this peak value, or the fraction of particles removed from the upper into the lower stream, increases during each cycle. These simulations illustrate that the "catch and release" effect is robust even in more "harsh" conditions where a portion of the adhesive nanoparticles are continuously brought back into the upper stream during the recovery stroke. In contrast, in the experimental device, released proteins will flow through the lower stream outlet port. However, similar to the experiment, about 95% of the adhesive nanoparticles are released into the lower phase by the ninth cycle (Fig.4) and this number continues to increase in subsequent cycles. This indicates that the catch and release system is expected to work in a qualitatively similar manner for a wide range of recycling conditions.

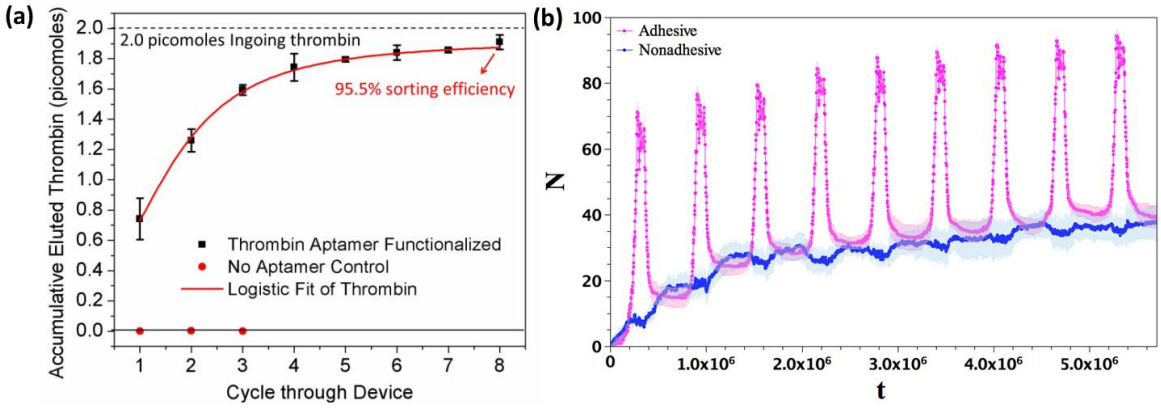

Figure 4. System performance in multiple oscillation cycles with recycling of the ingoing solution. *(a) Thrombin collected from recycling of ingoing solution. Thrombin (2 picomoles) was pumped into the top layer of the microfluidic channel. After each actuation of the system, the bottom solution was collected and the top layer was recycled through the channel. Eluted thrombin was quantified by ELISA. The cumulative amount of eluted thrombin after each actuation is calculated and plotted. The control system containing no aptamer shows no measurable elution of thrombin; the aptamer-functionalized system shows elution of 95.5% of the ingoing thrombin in the bottom layer after eight cycles of capture-and-release. The near quantitative recovery of the ingoing thrombin suggests that the surfaces of the microfluidic channel and the hydrogel have very little nonspecific association with the target protein. (b) Computer simulations showing the evolution of the number of particles in the lower stream, N, for adhesive nanoparticles (in magenta) and non-adhesive nanoparticles (in blue) for a total of 200 particles (100 of each type) during nine oscillation cycles.*

To experimentally test the system's ability to selectively capture thrombin from a mixture of proteins, a solution containing a mixture of thrombin and transferrin, an iron-binding plasma glycoprotein, as well as a mixture of thrombin and bovine serum albumin (BSA) was introduced into the microfluidic channel with aptamer-decorated and unfunctionalized microstructures, as well as microstructures functionalized with a scrambled DNA sequence that does not bind thrombin.[32, 37] The resulting top and bottom fluids were collected separately and analyzed by PAGE gel. The thrombin aptamer-decorated system selectively captured thrombin from the top fluid and released it in the bottom solution for both mixtures, while both BSA and transferrin were retained in the top layer; additionally, all the thrombin, transferrin and BSA were retained in the top layer in the control systems (Fig.5a, b). To further test the efficacy of filtrating specific protein from a more complex, blood-like environment, human serum containing thrombin was introduced in the system in a similar way with thrombin successfully sorted out (Fig. 5c), confirming the design's generality and applicability to sorting biomolecules from mixtures. It is evident that there is very little non-specific interaction of the device with the solution mixture, where non-specific fouling is reduced by constant flow of biomolecules through the device.

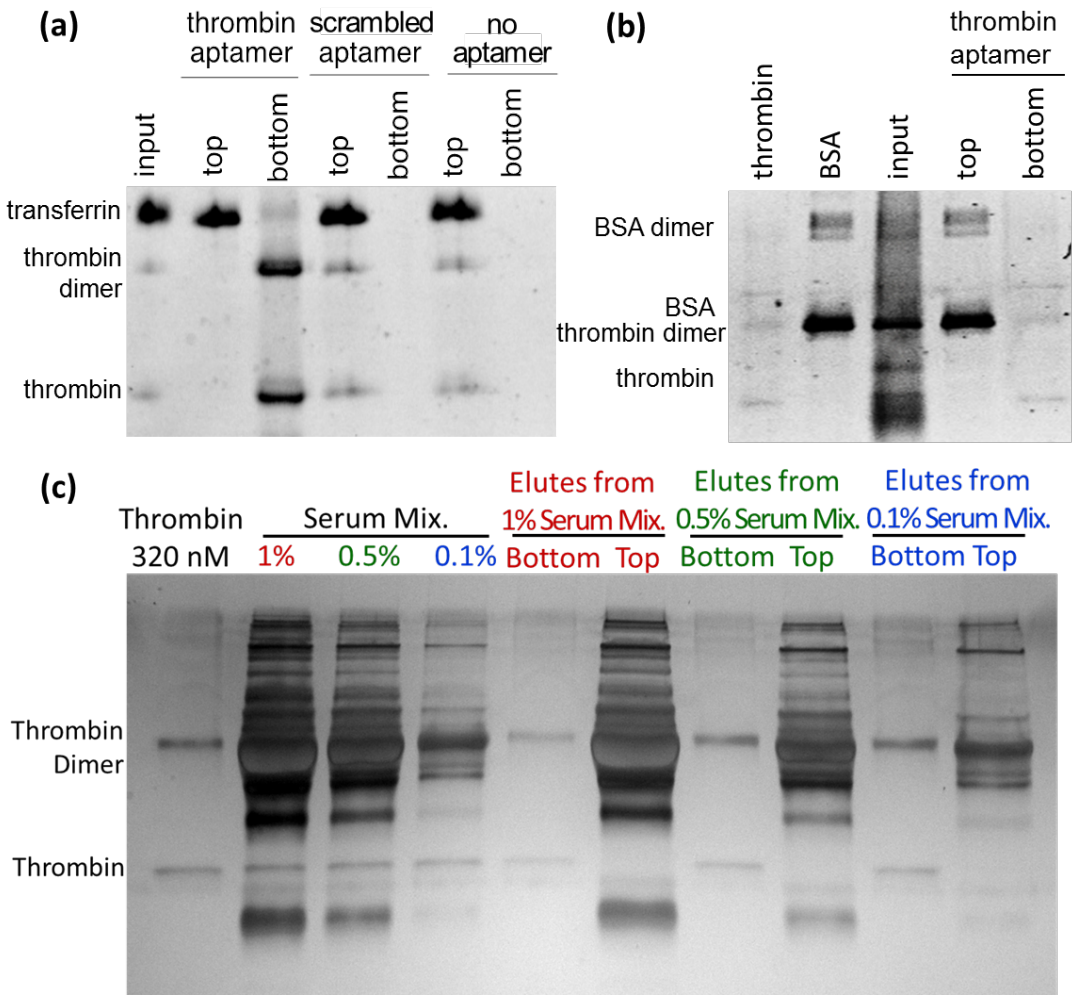

Figure 5. A PAGE gel was used to analyze the components of the top and bottom solutions after cycling through the microfluidic systems. *A solution of thrombin mixed with different interfering non-target protein(s), including (a) transferrin, (b) bovine serum albumin (BSA), and (c) 1%, 0.5% and 0.1% human serum, was pumped into the top layer of the microsystem. The top layer was recycled for multiple times through the channel over repeated hydrogel actuations and was collected after the final actuation, while solutions from the bottom layer were collected after each actuation and pooled. In a microsystem functionalized with a thrombin aptamer, thrombin was eluted specifically from the bottom layer, while the interfering non-target protein(s), i.e. transferrin, BSA, and other proteins in serum, were retained in the top layer, despite repeated cycling of the top layer solution. In (a), in control experiments where microstructures were either unfunctionalized or decorated with a nonbinding scrambled DNA sequence, both thrombin and transferrin were retained in the top layer.*

Each component of our chemo-mechanically modulated system can be individually tailored to produce a desired output. For example, the hydrogel composition, microstructure material, geometry, and array dimensions, or functionalization of the microstructure tips can all be adjusted. As one example, the hydrogel composition can be

changed to alter its response time or its degree of swelling (and, correspondingly the tilt angle of the microfins, θ_{low}). With the aid of the computer simulations, we can predict the influence of these parameters on the system's performance. For instance, we show that for a given interface height, there is a well-defined range of θ_{low} values that results in the efficient catch-and-release; however, an increase in θ_{low} above the threshold value results in a rapid decrease in the fraction of adhesive particles released into the lower stream (Fig.S6). We find the system's performance to be relatively insensitive to τ_{down}. Finally, our simulations show that varying the position of the fluid-fluid interface can also be used to adjust the system's efficiency and indicate an optimal interface height for a given fin length (See Section 5.2.1 of SI).

Conclusions

We have designed and tested a miniature bio-inspired microfluidic system that uniquely couples pH-manipulated microfin actuation with pH-dependent aptamer unfolding/refolding for biomolecule catch-transport-release, offering non-destructive separation of specific molecules from a complex solution through a robust and tunable chemo-mechano-biochemical process. Additionally, the reversibility of hydrogel swelling and aptamer folding allows for repeated processing of a single input solution, enabling multiple recycling and high capture of the target molecules from the initial mixture. Compared to other small-volume biomolecule sorting systems that rely on external electric fields,[38] IR,[39] magnetic fields,[7, 40] require chemical modifications of the biomolecules of interest,[41] lead to only single-time use of a given set-up,[42] or require a series of sequential steps for the release of the biomolecule and/or reuse of the device,[32, 43] our system can exploit coupled chemistries in a microfluidic channel to yield both efficient (minimal steps) and effective (recovery of almost all of the target biomolecule from solution) output.

The reversible chemo-mechanical modulation character of this system makes it suitable for numerous applications that require separation of microliter samples for downstream analysis with low turnaround time. The variability and tunability of the hydrogel, aptamer binding strength, geometry and material of the microstructure, and flow

characteristics make this system a broad-based, customizable platform for multiple applications. The microstructures can be functionalized with a diverse array of environmentally-responsive aptamers, antibodies, catalysts, or small molecules, in principle allowing attachment of several target molecules. SELEX allows for easy identification of aptamer sequences that can target a broad range of proteins and molecules under a variety of conditions, allowing for selection of binding that is responsive to factors such as pH, temperature, salt, *etc*.[44-46] As research on aptamers expands and modification of aptamers with appropriate ionizable groups becomes increasingly viable[47, 48] for pH-dependent behavior, our platform can be used for such targets, as well. In addition, G-quartet binding, which is involved in the aptamer-thrombin binding in this work, is evident in many other sequence-target configurations, making our proof-of-concept likely applicable to these other biomolecules as well.[49, 50] The chemistry of the hydrogel can be tuned to achieve stimuli-responsive sorting at various conditions, as hydrogels can be made to respond to temperature, light, electric/magnetic field, ionic concentration, etc. Such a broad spectrum of multiple chemistries possible within a single, dynamic system could find further applications not only in biomedical fields, but also inorganic and/or synthetic chemistry fields for microfluidic analysis of chemical binding/releasing and sensing, with the purposes of determining chemical purity, chirality, molecular binding kinetics or affinity in different environments.

Materials and Methods

Chemicals: Acrylamide (AAm), acrylic acid (AAc), dodecyl acrylate, glycidyl methacrylate (GMA), 2-hydroxy-4-(2-hydroxyethoxy)-2-methylpropiophenone (Irgacure 2959, photoinitiator), (tridecafluoro-1,1,2,2-tetrahydrooctyl)trichlorosilane and dithiothreitol were purchased from Sigma-Aldrich (St. Louis, MO) and used as received. Polydimethylsiloxane (PDMS) (Dow-Sylgard 184) was purchased from Ellsworth (Germantown, WI) and UVO-114 was purchased from Epoxy Technology (Billerica, MA). For ELONA measurements, streptavidin-coated 96-well plates, clear, were ordered from Thermo Scientific (Rockford, Illinois). Anti-thrombin HRP Polyclonal antibody conjugate for ELONA assays was purchased from Thermo Scientific (Rockford, Illinois). A solution of TMB with hydrogen peroxide was purchased from Thermo Scientific (Rockford, Illinois). For thrombin detection, a thrombin-specific ELISA kit was purchased from Antibodies-online.com (Atlanta, Georgia). Human plasma thrombin was purchased from EMD Millipore Chemicals (Billerica, MA). Human transferrin, 98%, and human serum from human male AB plasma were purchased from Sigma-Aldrich (Allentown, PA).

DNA synthesis: Oligonucleotides were purchased from Integrated DNA Technologies (Coralville, IA) or synthesized on a PerSeptive Biosystems Expedite 8909 DNA synthesizer using reagents and phosphoramidites purchased from Glen Research (Sterling, VA). Oligonucleotides were synthesized and deprotected according to manufacturer's protocols and purified by either OPC cartridge (ABI) or by reverse-phase high pressure liquid chromatography (HPLC, Agilent 1200) using a C18 stationary phase and an acetonitrile/100 mM trimethylammonium acetate gradient. Non-commercial oligonucleotides were characterized by LC/ESI-MS with reverse phase separation on an alliance 2695 (Waters) HPLC system using a UPLC BEH C18 column (1.7 μM, 2.1 x 50 mm) stationary phase and a 6 mM aqueous triethylammonium bicarbonate/methanol mobile phase interfaced to a Q-Tof Micro mass spectrometer (Waters). Thrombin aptamer: 5'-GGTTGGTGTGGTTGG-thiol C6 SS -3' using the 3' thiol C6 modified CPG resin (Glen Research). Biotinylated thrombin aptamer: 5'-GGTTGGTGTGGTTGG-biotinTEG -3' using the

3’ biotinTEG resin (Glen Research). Scrambled thrombin aptamer: 5’-GGTGGTGGTTGTGGT-thiol C6 SS –3’. Thrombin apatmer probe: 5'-/5Cy5/ CCA ACC ACA CCA ACC -3'.

Deprotection of Aptamer Disulfide to Free Thiol: Purified DNA aptamers were diluted in phosphate buffered saline (PBS, pH 7.2) and combined with 0.1 volumes of 1M dithiothreitol (DTT, Sigma Alrich). This mixture was incubated at room temperature for 30 minutes before the free 3’-thiol linked aptamer was recovered by ethanol precipitation.

Functionalization of Microstructure Tips with Aptamer: A PDMS block was used to stamp 3’thiol-modified aptamers onto the epoxy microfins. 20 μL of a 10mM aptamer solution was applied to a small area of PDMS, which was then carefully placed on top of the oxygen-plasma treated epoxy structures and left to incubate overnight at 4°C. Thorough washing of the sample removed excess, unbound aptamer from the microstructured sample.

Biomolecule sorting and collection in microfluidic system: 100μL of 500nM BSA blocking solution was flowed through the channel. Subsequently, 100μL of thrombin solution in pH 6.3 buffer was flowed in the top layer while 100μL of pH 7.2 buffer was flowed in the bottom layer. To determine the sorting capacity of the microfluidic system, 100μL of different initial thrombin concentrations, 5nM, 10nM, 20nM, 40nM, 80nM was flowed in the top layer. 100μL of outgoing solution was collected from the top layer. The flow rate was 10μL/min for the top fluid and 30μL/min for the bottom fluid, respectively. For biomolecule release, 100μL of pH 6.3 buffer containing no biomolecules was flowed in the top layer and 100μL of pH 3.2 buffer was flowed in the bottom layer to contract the hydrogel and release bound biomolecules. 100μL of outgoing solution was collected from the bottom layer. Collected aliquots were diluted and analyzed with ELISA (described below). To determine the sorting ability with multiple sorting cycles of a given thrombin solution, the process described was repeated eight times whereby the same initial ingoing thrombin solution in the first cycle was reintroduced through the top layer each subsequent cycle.

PAGE experiment for selectivity test: Fractions from the top and bottom layers of the channel were collected and pooled after several actuations conducted upon an ingoing mixture solution containing 20 nM thrombin and 20 nM transferrin, 20 nM bovine serum albumin (BSA), or 1%, 0.5% and 0.1% human serum. The top layer eluting solutions were re-pumped in the microsystem for multiple times, 8 times for transferrin- and BSA-containing mixture and 40, 20, 10 times for 1%, 0.5% and 0.1% serum mixtures. Fractions were concentrated by lyophilization, redissolved in 1x NuPAGE protein loading buffer (Invitrogen), heated to 95˚C for 5 minutes and analyzed by electrophoresis (12% NuPAGE gel (Invitrogen), 200V, 45 min) The gel was subsequently stained with Sypro Ruby (Sigma) and imaged on a ChemiImager.

ELISA experiment for quantitative measurement of thrombin concentration:

To measure the amount of thrombin eluted from the top and bottom layer of the microfluidic channel, a thrombin-specific ELISA kit (Fisher Scientific) was used. Standard curves were made of thrombin at known concentrations in the relevant pH buffers, pH 6.3 and pH 3.2. Aliquots of collected solution from the top and bottom layer were diluted appropriately and dispensed along with the standard solutions onto a microplate pre-coated with a monoclonal antibody specific for thrombin. After incubation of the thrombin solutions for 2 hours, the unbound thrombin was washed away. A biotinylated polyclonal thrombin antibody was then incubated on the microplate for 1 hour. After washing away excess, unbound anti-thrombin, streptavidin peroxidase conjugate was deposited on the microplate to recognize the bound anti-thrombin antibody and left to incubate for 30 minutes. After washing away excess streptavidin peroxidase conjugate, a chromogenic substrate, TMB, was added to the microplate and incubated for 10 minutes after which 0.5N HCl solution was added to stop the chromogen substrate reaction and the absorbance was quantified at 450nm. The intensity of absorption at 450 nm for collected thrombin was compared to a standard curve to calculate the amount of collected thrombin on the SpectraMax M5 from Molecular Devices.

Acknowledgments: This work was supported by Department of Energy under the Award #: DE-SC0005247. We thank Marie Krogsgaard and Catlin Howell for the help with XPS characterization of the aptamer functionalization of the microstructures.

References:

1. Fratzl, P. & Barth, F.G. Biomaterial Systems for Mechanosensing and Actuation. *Nature* **462**, 442-448 (2009).
2. Stuart, M.A.C., Huck, W.T.S., Genzer, J., Mueller, M., Ober, C., Stamm, M., Sukhorukov, G.B., Szleifer, I., Tsukruk, V.V., Urban, M., Winnik, F., Zauscher, S., Luzinov, I. & Minko, S. Emerging Applications of Stimuli-responsive Polymer Materials. *Nature Materials* **9**, 101-113 (2010).
3. Cabodi, M., Chen, Y.F., Turner, S.W.P., Craighead, H.G. & Austin, R.H. Continuous Separation of Biomolecules by the Laterally Asymmetric Diffusion Array with Out-of-plane Sample Injection. *Electrophoresis* **23**, 3496-3503 (2002).
4. Cho, E.J., Collett, J.R., Szafranska, A.E. & Ellington, A.D. Optimization of Aptamer Microarray Technology for Multiple Protein Targets. *Analytica Chimica Acta* **564**, 82-90 (2006).
5. Eigen, M. & Rigler, R. Sorting Single Molecules - Application to Diagnostics and Evolutionary Biotechnology. *Proceedings of the National Academy of Sciences of the United States of America* **91**, 5740-5747 (1994).
6. Song, Y.A., Hsu, S., Stevens, A.L. & Han, J.Y. Continuous-flow pl-based Sorting of Proteins and Peptides in a Microfluidic Chip Using Diffusion Potential. *Analytical Chemistry* **78**, 3528-3536 (2006).
7. Fu, J., Mao, P. & Han, J. Artificial Molecular Sieves and Filters: A New Paradigm for Biomolecule Separation. *Trends in Biotechnology* **26**, 311-320 (2008).
8. He, X., Li, C., Chen, F.G. & Shi, G.Q. Polypyrrole microtubule actuators for seizing and transferring microparticles. *Adv Funct Mater* **17**, 2911-2917 (2007).
9. Levy-Nissenbaum, E., Radovic-Moreno, A.F., Wang, A.Z., Langer, R. & Farokhzad, O.C. Nanotechnology and Aptamers: Applications in Drug Delivery. *Trends in Biotechnology* **26**, 442-449 (2008).
10. Sengupta, S., Patra, D., Ortiz-Rivera, I., Agrawal, A., Shklyaev, S., Dey, K.K., Cordova-Figueroa, U., Mallouk, T.E. & Sen, A. Self-powered Enzyme Micropumps. *Nature Chemistry* **6**, 415-422 (2014).
11. Koga, S., Williams, D.S., Perriman, A.W. & Mann, S. Peptide-nucleotide microdroplets as a step towards a membrane-free protocell model. *Nature Chemistry* **3**, 720-724 (2011).
12. Maitz, M.F., Freudenberg, U., Tsurkan, M.V., Fischer, M., Beyrich, T. & Werner, C. Bio-responsive Polymer Hydrogels Homeostatically Regulate Blood Coagulation. *Nature Communications* **4** (2013).
13. Rodriguez-Llansola, F. & Meijer, E.W. Supramolecular Autoregulation. *Journal of the American Chemical Society* **135**, 6549-6553 (2013).

14. Roglin, L., Lempens, E.H.M. & Meijer, E.W. A Synthetic "Tour de Force": Well-Defined Multivalent and Multimodal Dendritic Structures for Biomedical Applications. *Angewandte Chemie-International Edition* **50**, 102-112 (2011).
15. Wang, J.B. & Feringa, B.L. Dynamic Control of Chiral Space in a Catalytic Asymmetric Reaction Using a Molecular Motor. *Science* **331**, 1429-1432 (2011).
16. Wilson, D.A., Nolte, R.J.M. & van Hest, J.C.M. Autonomous movement of platinum-loaded stomatocytes. *Nature Chemistry* **4**, 268-274 (2012).
17. He, X., Aizenberg, M., Kuksenok, O., Zarzar, L., Shastri, A., Balazs, A.C. & Aizenberg, J. Synthetic Homeostatic Materials Displaying Chemo-mechano-chemical Self-regulation. *Nature* **487**, 214-218 (2012).
18. de Ruiter, G. & van der Boom, M.E. Surface-Confined Assemblies and Polymers for Molecular Logic. *Accounts of Chemical Research* **44**, 563-573 (2011).
19. Krieg, E., Weissman, H., Shirman, E., Shimoni, E. & Rybtchinski, B. A Recyclable Supramolecular Membrane for Size-selective Separation of Nanoparticles. *Nature Nanotechnology* **6**, 141-146 (2011).
20. Hirokawa, N. Kinesin and Dynein Superfamily Proteins and the Mechanism of Organelle Transport. *Science* **279**, 519-526 (1998).
21. Cho, E.J., Lee, J.W. & Ellington, A.D. in Annual Review of Analytical Chemistry, Vol. 2 241-264 (Annual Reviews, Palo Alto; 2009).
22. Mosing, R.K. & Bowser, M.T. Microfluidic Selection and Applications of Aptamers. *Journal of Separation Science* **30**, 1420-1426 (2007).
23. Jeong, B. & Gutowska, A. Lessons From Nature: Stimuli-responsive Polymers and Their Biomedical Applications. *Trends in Biotechnology* **20**, 305-311 (2002).
24. Yerushalmi, R., Scherz, A., van der Boom, M.E. & Kraatz, H.B. Stimuli Responsive Materials: New Avenues Toward Smart Organic Devices. *Journal of Materials Chemistry* **15**, 4480-4487 (2005).
25. Krieg, E., Shirman, E., Weissman, H., Shimoni, E., Wolf, S.G., Pinkas, I. & Rybtchinski, B. Supramolecular Gel Based on a Perylene Diimide Dye: Multiple Stimuli Responsiveness, Robustness, and Photofunction. *Journal of the American Chemical Society* **131**, 14365-14373 (2009).
26. Macaya, R.F., Schultze, P., Smith, F.W., Roe, J.A. & Feigon, J. Thrombin-binding DNA Aptamer Forms A Unimolecular Quaruplex Structure in Solution. *Proceedings of the National Academy of Sciences of the United States of America* **90**, 3745-3749 (1993).
27. Tasset, D.M., Kubik, M.F. & Steiner, W. Oligonucleotide Inhibitors of Human Thrombin That Bind Distinct Epitopes. *Journal of Molecular Biology* **272**, 688-698 (1997).
28. Rathi, L.S., Stephen C. Chapin, and Patrick S. Doyle Aptamer-Functionalized Microgel Particles for Protein Detection. *Analytical Chemistry* **83**, 9138–9145 (2011).
29. Cheng, M.M.C., Cuda, G., Bunimovich, Y.L., Gaspari, M., Heath, J.R., Hill, H.D., Mirkin, C.A., Nijdam, A.J., Terracciano, R., Thundat, T. & Ferrari, M. Nanotechnologies for Biomolecular Detection and Medical Diagnostics. *Current Opinion in Chemical Biology* **10**, 11-19 (2006).
30. Guo, M.T., Rotem, A., Heyman, J.A. & Weitz, D.A. Droplet Microfluidics for High-throughput Biological Assays. *Lab on a Chip* **12**, 2146-2155 (2012).

31. Martinez, A.W., Phillips, S.T., Whitesides, G.M. & Carrilho, E. Diagnostics for the Developing World: Microfluidic Paper-Based Analytical Devices. *Analytical Chemistry* **82**, 3-10 (2010).
32. Dick, L.W. & McGown, L.B. Aptamer-enhanced Laser Desorption/ionization for Affinity Mass Spectrometry. *Analytical Chemistry* **76**, 3037-3041 (2004).
33. He, X., Friedlander, R.S., Zarzar, L.D. & Aizenberg, J. Chemo-Mechanically Regulated Oscillation of an Enzymatic Reaction. *Chemistry of Materials* **25**, 521-523 (2013).
34. Bhattacharya, A. & Balazs, A.C. Stiffness-modulated Motion of Soft Microscopic Particles Over Active Adhesive Cilia. *Soft Matter* **9**, 3945-3955 (2013).
35. Hianik, T.O., V.; Sonlajtnerova, M. & Grman, I. Influence of Ionic Strength, pH and Aptamer Configuration for Binding Affinity to Thrombin. *Bioelectrochemistry* **70**, 127-133 (2007).
36. Baldrich, E., Restrepo, A. & O'Sullivan, C.K. Aptasensor Development: Elucidation of Critical Parameters for Optimal Aptamer Performance. *Analytical Chemistry* **76**, 7053-7063 (2004).
37. Bock, L.C., Griffin, L.C., Latham, J.A., Vermaas, E.H. & Toole, J.J. Selection of Single-stranded DNA Molecules That Bind and Inhibit Human Thrombin. *Nature* **355**, 564-566 (1002).
38. Zeng, Y. & Harrison, D.J. Self-assembled Colloidal Arrays as Three-dimensional Nanofluidic Sieves for Separation of Biomolecules on Microchips. *Analytical Chemistry* **79**, 2289-2295 (2007).
39. Arakawa, T., Shirasaki, Y., Aoki, T., Funatsu, T. & Shoji, S. Three-dimensional Sheath Flow Sorting Microsystem Using Thermosensitive Hydrogel. *Sens. Actuators A: Physical* **135**, 99-105 (2007).
40. Doyle, P.S., Bibette, J., Bancaud, A. & Viovy, J.L. Self-assembled Magnetic Matrices for DNA Separation Chips. *Science* **295**, 2237-2237 (2002).
41. Pedersen, J., Petersen, G.E., Lauritzen, C. & Arnau, J. Current Strategies for the Use of Affinity Tags and Tag Removal for the Purification of Recombinant Proteins. *Protein Expression and Purification* **48**, 1-13 (2006).
42. Chen, L., Liu, X., Su, B., Li, J., Jiang, L., Han, D. & Wang, S. Aptamer-Mediated Efficient Capture and Release of T Lymphocytes on Nanostructured Surfaces. *Advanced Materials* **23**, 4376-4380 (2011).
43. Zhang, L., Chatterjee, A. & Leung, K.T. Hydrogen-Bond-Mediated Biomolecular Trapping: Reversible Catch-and-Release Process of Common Biomolecules on a Glycine-Functionalized Si(111)7 x 7 Surface. *Journal of Physical Chemistry Letters* **1**, 3385-3390 (2010).
44. Jayasena, S.D. Aptamers: An emerging class of molecules that rival antibodies in diagnostics. *Clinical Chemistry* **45**, 1628-1650 (1999).
45. Wochner, A., Menger, M., Orgel, D., Cech, B., Rimmele, M., Erdmann, V.A., & Glokler, J. A DNA Aptamer with High Affinity and Specificity for Therapeutic Anthracyclines. *Anal. Biochem.* **373**, 34-42 (2008).
46. Zhai, G., Iskander, M., Barilla, K., & Romaniuk, P.J. Characterization of RNA Aptamer Binding by the Wilms' Tumor Suppressor Protein WT1. *Biochemistry* **40**, 2032-2040 (2001).
47. Lin, Y., Qiu, Q., Gill, S.C., & Jayasena, S.D. Modified RNA Sequence Pools for In Vitro Selection. *Nucleic Acids Research* **22**, 5229-5234 (1994).

48. Schurer, H., Stembera, K., Knoll, D., Mayer, G., Blind, M., Forster, H., Famulok, M., Welzel, P., & Hahn, U. Aptamers That Bind to Antibiotic Moenomycin A. *Bioorg. Med. Chem.* **9**, 2557-2563 (2001).
49. Li, T., Shi, L., Wang, E., & Dong, S. Multifunctional G-Quadruplex Aptamers and Their Applications to Protein Detection. *Chem. Eur. J.* **15**, 1036-1042 (2009).
50. Fujita, H., Imaizumi, Y., Kasahara, Y., Kitadume, S., Ozaki, H., Kuwahara, M., & Sugimoto, N. Structural and Affinity Analyses of G-Quadruplex DNA Aptamers for Camptothecin Derivatives. *Pharmaceuticals* **6**, 1082-1093 (2013).